MEASUREMENT OF INPUT IMPEDANCE OF AN ACOUSTIC BORE WITH APPLICATION TO BORE RECONSTRUCTION

Maarten van Walstijn Department of Physics and Astronomy, University of Edinburgh, Edinburgh
Murray Campbell Department of Physics and Astronomy, University of Edinburgh, Edinburgh
David Sharp Department of Environmental and Mechanical Engineering, The Open University, Walton Hall, Milton Keynes

Abstract: This paper reports on the development of a method for experimentally determining the input impedance of an acoustic bore. The method and the experimental setup are designed having in mind the requirements associated with the possibility of applying high-resolution bore reconstruction algorithms to the measurement data. As such, the measurement bandwidth at which the method needs to produce accurate data is much larger than that in previously developed experimental methods for determination of input impedance. In the paper, we discuss the details of the design of the experimental setup and the initial results obtained, as well as the particular problem that occurs when measuring an acoustic bore whose input diameter is different from the exit diameter of the measurement head.

1. INTRODUCTION

Bore reconstruction is a useful tool for analysis of the relation between the geometrical shape of an acoustic bore and its acoustic response. Algorithms for bore reconstruction typically start from the impulse response of an acoustic bore, which can be measured directly in the time-domain via pulse reflectometry techniques (see for example [1]). However, the bore may in principle also be reconstructed from a frequency-domain description, such as the input impedance, which can be measured directly in the frequency-domain. If the reconstruction algorithm is deterministic, as opposed to algorithms that are based on optimisation (see for example [2]), the frequency bandwidth is proportional to the axial resolution of the reconstruction profile. For instance, in order to obtain an axial resolution of 4 mm, the impedance measurement method must be accurate up to about 20 kHz. Previously developed impedance measurement methods, such as those employing a capillary, are often accurate only at low frequencies; thus alternative methods are required if a larger bandwidth is to be measured. One of the key-features of a suitable method is that it should be insensitive to the influences of local non-propagating modes, which are typically significant at short wavelengths.

In this paper we propose a method that measures the "plane-wave input impedance", which corresponds to the corner-element of the multimodal impedance matrix described by Pagneux et al. [3]. In the mathematical description employed by Pagneux et al., the acoustic variables are denoted as vectors, with each vector element representing an axisymmetrical mode. For example, the pressure is denoted by the vector $\mathbf{p}$, where $\mathbf{p}_0$ is the plane-wave component of the pressure, and $\mathbf{p}_1$ is the pressure component of the (0,1) *mode*. The quantity acoustic impedance,

which relates pressure to volume velocity, takes on a matrix-form in this notation, thus the corner-element $\mathbf{Z}_{00}$ is the plane-wave component of the impedance matrix $\mathbf{Z}$. We emphasise that for the purpose of bore reconstruction, one specifically needs to find $\mathbf{Z}_{00}$ (rather than simply the ratio of total pressure over total volume velocity), especially when non-propagating modes are excited in the reference plane.

The experimental method used in the present study is based on the "two-microphone-three-calibration (TMTC) method" developed by Gibiat and Laloë [4]. A brief summary of the TMTC method is given in the first subsection of section 2. In the remainder of section 2, we discuss various features of the method that are important with respect to the design of the experimental setup, such as the restrictions that the dimensions of the calibration objects put on the calibration procedure.

In section 3, the results of initial measurements are presented and discussed. The impedances of two cylindrical pipes are measured, one of which presents a case in which non-propagating modes are excited at the reference plane at which the impedance is measured.

2 THE TMTC METHOD

2.1 General Description of the Method

Figure 1 shows a sketch of the experimental setup of the TMTC method. During an experiment, a speaker is used to excite the air in the measurement head, while the two microphones placed in the wall record the pressure at two different locations in the measurement head. The method is designed to measure the impedance at the reference plane, which equals that of the boundary condition at that position (i.e. the impedance of the object placed on the measurement head). If we may assume that there are no higher modes propagating throughout the system in the frequency range of interest, the relationship between the microphone signals and the pressure p and volume velocity U in the reference plane may be expressed as:

$$s_1 = \alpha p + \beta Z_0 U, \tag{1}$$
$$s_2 = \gamma p + \delta Z_0 U, \tag{2}$$

where α, β, γ, and δ are unknown parameters that depend on the microphone admittances and the acoustical paths between the microphones and the reference plane. It can be shown that from these equations one can derive an expression for the input impedance in the reference plane:

$$Z = p / U = Z_0 (Ay + B) \cdot (y - y_0)^{-1}, \tag{3}$$

where Z_0 is the characteristic impedance of the measurement head in the reference plane, $y = s_2 / s_1$ is the ratio of measured signals, and

$$A = -\beta / \alpha, \qquad B = \delta / \alpha, \qquad y_0 = \gamma / \alpha. \tag{4}$$

The parameters A, B, and y_0 can be thought of as the three dimensionless calibration parameters that have to be determined at each frequency before carrying out a measurement of an unknown impedance. This calibration is realised via measurements with three systems of known impedances. As one of the calibration impedances, one may simply close off the measurement head at the reference plane; the admittance in the reference plane is in that case approximately zero. Measuring the ratio y then immediately gives the value of the calibration parameter y_0 (see equation (3)). Next, two acoustic cavities of known impedances Z' and Z'' are placed on the

measurement head, and the corresponding values y' and y'' are measured. From equation (3), the following relations are then obtained:

$$Z'(y' - y_0) = Z_0 (Ay' + B), \quad (5)$$
$$Z''(y'' - y_0) = Z_0 (Ay'' + B). \quad (6)$$

This system of two linear equations has the solutions:

$$A = [Z'(y' - y_0) - Z''(y'' - y_0)] \cdot [Z_0 (y' - y'')]^{-1}, \quad (7)$$
$$B = [Z'' y' (y'' - y_0) - Z' y'' (y' - y_0)] \cdot [Z_0 (y' - y'')]^{-1}. \quad (8)$$

Next, the acoustic bore under study is placed on the measurement head, and the corresponding ratio y is measured. Using equations (5), (7), and (8), the unknown impedance Z is then derived as:

$$Z = [Z' (y' - y_0)(y - y'') + Z'' (y'' - y_0)(y' - y)] \cdot [(y - y_0)(y' - y'')]^{-1}. \quad (9)$$

Since the microphones are positioned in a cylindrical tube, one may assume that only a single propagation mode (i.e. the plane wave mode) is measured. Hence the variables p and U in equations (1) and (2) are in fact the "plane wave components" of the actual total pressure and volume velocity in the reference plane. Within the mathematical description of multi-modal systems as presented by Pagneux et al., the measured impedance Z can be thought of as the corner-element $\mathbf{Z}_{00}$ of the impedance matrix $\mathbf{Z}$ at the reference plane. Of course, when no non-propagating modes are active in this plane, $\mathbf{Z}_{00}$ equals the ratio of the total pressure and the total volume velocity.

2.2 Excitation

A speaker is mounted at the end of the measurement head and driven with a sinusoidal signal in order to excite the air inside the measurement head. The main part of the head is cylindrical, and a short conical section connects the speaker with this cylinder to ensure a better transmission of signal energy towards the reference plane. The signal that is sent to the speaker is a chirp that is designed to have approximately uniform spectral amplitude at the microphone that is positioned most closely to the reference plane. This "calibrated" chirp signal is calculated from the signal s_1 that is recorded after sending a normal chirp with uniform amplitude to the speaker, with the measurement head terminated anechoically. In order to suppress transient effects, the chirp is faded in before it reaches the minimum frequency f_{min} to be measured and faded out after reaching the maximum frequency f_{max}. Figure 2 shows the "calibrated" chirp signal and the resulting signal recorded at the first microphone, together with the corresponding magnitude spectra with f_{min} = 1 kHz and f_{max} = 8 kHz.

2.3 Measurement Head

The lowest cut-off frequency of the cylindrical bore of radius a is that of the (1,0) mode [5]:

$$f_c = 1.84\, c / a, \quad (10)$$

where c is the wave velocity. Hence for measurement of a single propagation mode in the measurement head up to frequency f_{max} = 20 kHz, the radius of the cylindrical part has to be smaller or equal to $(1.84c) / f_{max} \approx 5$ mm. Because (1) the viscothermal losses are larger for

smaller radii and (2) the signal to noise ratio (SNR) of the microphone signals is better with small losses than with large losses, the radius should be chosen only slightly below this "maximum value". Furthermore, the distance L_1 between the reference plane and the first microphone should be sufficiently large to avoid "contamination" of the microphone signal with non-propagating mode wave components. Taking into account these prerequisites, the dimensions a = 4.6 mm and L_1 = 32 mm were chosen. From theory one can deduce that the amplitude of the mode (1,0) is then about 20 dB lower at the microphone than in the reference plane at 20 kHz, and more than 100 dB lower at frequencies below 10 kHz. In practice, this means that the microphones measure a sufficiently "clean" plane-wave signal.

2.4 Calibration Objects

As explained in [4], the dimensions of the objects used for calibration need to be chosen carefully. That is, if the impedance magnitude is relatively large at a certain frequency, the derivation of the calibration parameters is problematic because the ratio y' measured will be similar to the ratio y_0 measured with the end of the measurement head closed off; in that case the same "answer" is fed twice into a system of three equations, and therefore the system of equations (7) and (8) becomes degenerate; this occurs at resonance frequencies of the calibration object. For example, with a short cylindrical cavity, the resonances occur whenever the length L' equals half the wavelength (or multiples of half the wavelength). Gibiat and Laloë solve this problem by using two cylindrical cavities of lengths L' = $\lambda/6$ and L'' = $\lambda/3$, each with a closed end, where λ is the wavelength. In our initial experiments, we employed a short cylindrical cavity as one of the calibration objects, and an anechoic tube of the same diameter as the cylindrical part of the measurement head as the other. The use of such an anechoic tube is potentially advantageous because its impedance is independent of frequency, thus the derivation of Z is not complicated by any resonances of this object.

2.5 Condition at the Reference Plane

Gibiat and Laloë define the input impedance as the ratio of the actual pressure and flow at the reference plane. This definition requires that there are no non-propagating modes excited at the reference plane. A practical consequence is that the acoustic bore under study must have a perfectly cylindrical entry of the same radius as the measurement head exit. Such a restriction strongly limits the applicability of the method. However, it is questionable whether this condition is really necessary. Even if non-propagating modes are active in the reference plane, the main formulas on which the method is based (i.e. equations (1) and (2)) still apply. The only problem is that in that case, the impedance that is derived with equation (9) is not what is generally known as the "plane wave impedance" of the object. For example, consider the measurement of an object with a cylindrical entry that is considerably wider than the measurement head (see figure (3)). If the calibration objects have the same diameter as the measurement head, the impedance derived with equation (9) is the corner element $\mathbf{Z}_{00}^{(1)}$ of the impedance matrix directly at the left-hand side of the reference plane, which according to multimodal theory is not the same as the corner element of the impedance matrix $\mathbf{Z}_{00}^{(2)}$ at the right-hand side of the reference plane [3]. It is the latter that equals the plane-wave impedance of the acoustic bore under study. This particular problem is discussed further in sections 3 and 4.

2.6 Microphone Placement

As explained in [4], the two microphones are best placed at a distance $\lambda/4$ from each other for a wavelength λ. For this reason, different combinations of microphones must be used for different frequency bands. Hence the setup must be designed such that the resulting microphone

distances cover a desired frequency bandwidth. An efficient way to achieve this involves aligning the microphones according to a "golden mean ratio" series. That is, if the *n*th microphone is placed at a distance d_n from the first microphone (the microphone nearest to the reference plane), then the $(n+1)$th microphone is placed at a distance $d_{n+1} = d_n/g$, where $g = 0.5 \cdot [\text{sqrt}(5) - 1]$ is the golden mean ratio. The main advantage of this arrangement is that with each added microphone, two new microphone distances (namely d_n and $d_n - d_{n-1}$) are created, which result in two new frequency ranges that are evenly spaced on a logarithmical scale. Taking into account that also distances close to certain multiples of $\lambda/4$ are suitable (i.e. d = 3/4 λ, 5/4 λ, 7/4 λ...), this concept can in theory be used to cover a range from 40 Hz to 20 kHz (see figure 4). The arrangement provides a gradual scale of distances that can be combined to measure a wide range of frequencies. We note that only the golden mean ratio leads to frequency ranges that are evenly spaced on a logarithmic scale. Each particular microphone distance measures wavelengths varying from 0.20λ to 0.32λ, and we expect this to be sufficiently close to the "optimum" wavelength 0.25λ in order to avoid numerical problems in the calibration procedure.

2.7 Calibration Parameters

As mentioned earlier, the calibration parameters A, B, and y_0 characterise the acoustical paths between the microphones and the reference plane. Hence these parameters are independent of the boundary condition provided at the reference plane. Therefore a theoretical estimate of these parameters can be made. For simplicity, the part of the measurement head that contains the microphones is assumed to be perfectly cylindrical. That is, any disturbances of a plane wave travelling through the cylinder due to the presence of the microphones are ignored. We also assume that both microphones have zero admittance at all frequencies. Under these assumptions, the parameters in equations (1) and (2) can be derived from the transmission-line theory equations as presented by Keefe [6]:

$$\alpha = \cosh(\Gamma L_1), \tag{11}$$
$$\beta = \sinh(\Gamma L_1), \tag{12}$$
$$\gamma = \cosh(\Gamma L_2), \tag{13}$$
$$\delta = \sinh(\Gamma L_2). \tag{14}$$

Substitution into equation (4) yields:

$$A = -\sinh(\Gamma L_1) / \cosh(\Gamma L_1), \tag{15}$$
$$B = \sinh(\Gamma L_2) / \cosh(\Gamma L_1), \tag{16}$$
$$y_0 = \cosh(\Gamma L_2) / \cosh(\Gamma L_1). \tag{17}$$

In practice it is useful to compare these theoretical values to the measured ones, in order to get insight at which frequencies an accurate calibration is performed.

3 FIRST RESULTS

At the current stage, only a few measurements have been carried out with the experimental setup. The impedance of two (closed) cylindrical pipes have been measured; pipe #1 is 437 mm long and has a 9.3 mm diameter, and pipe #2 is 238 mm long and has a 18.8 mm diameter. For both pipes, the three reference impedances were those corresponding to (1) the end of the measurement head closed off, (2) a short cylindrical section (L' = 50 mm) of the same diameter as the measurement cylinder, and (3) an anechoic tube (L'' = 30 m, with sound-absorbing foam inserted at the end), also of the same diameter as the measurement cylinder. The measurements

were carried out using two different microphone distances (d = 37 mm and d = 59 mm). For a measurement using microphone distance d, we may expect problems at and around the frequency $f_d = c / (2d)$, because in that case the microphone distance is close to half the wavelength; for a standing wave, the two microphones then record approximately identical signals. For d = 37 mm and d = 59 mm, these frequencies are f_d = 4635 Hz and f_d = 2906 Hz, respectively. Similar numerical problems occur when d is close to a multiple of $\lambda/2$, thus at and around frequencies that are multiples of f_d. As explained in section 2.4, further problems arise at the resonance frequencies of the short calibration tube, which are positioned at multiples of $f' = c/(2L') \approx 3431$ Hz.

Figure 5 shows the three calibration parameters as a function of frequency, as obtained using the microphone distance d = 59 mm. For comparison, the theoretical values (equations (15), (16), and (16)) are also plotted. One can clearly notice that the parameter y_0 is hardly affected by any possible numerical complications; the discrepancy between theory and experiment can be attributed to the simplifying assumptions. On the other hand, the parameters A and B are clearly not well defined at and round the expected problem-frequencies. In order to obtain a well-defined calibration at these frequencies, one has to use a variety of different microphone distances and calibration objects, as explained in sections 2.6 and 2.4.

Figure 6 shows the results obtained for pipe #1. For comparison, the impedance as calculated from plane wave theory is also plotted. As for the calibration parameters A and B, the measured impedance closely approximates the theoretical curve, except at the frequency areas where numerical problems are expected. In fact, the fit is better than for A and B, since no simplifying assumptions are made about the effect that the microphones have on the wave propagation in the measurement head.

The measured impedance curve for pipe #2 is plotted in figure 7. As with pipe #1, the measured result does not match well with the theoretical result at the expected frequencies. However, in this case the discrepancy is also significant at other frequencies. In particular, many of the "impedance troughs" appear to be misaligned. Since this effect is significantly less strong with pipe #1, these "unexpected discrepancies" are likely to be due to the discontinuity at the reference plane with measuring pipe #2. If this is indeed the case, a possible explanation is that, as discussed in section 2.5, the method measures the impedance at the input side of the reference plane. Referring to figure (3), the measured impedance is the corner element $\mathbf{Z}_{00}^{(1)}$ of the impedance matrix $\mathbf{Z}^{(1)}$. It makes sense that the discrepancy due to this effect is larger at the troughs than at the peaks; at a plane-wave anti-resonance of the cylindrical bore under study, there is a $\mathbf{p}_0$ anti-node at the closed end and a $\mathbf{p}_0$ node at the reference plane, while at a resonance we have a $\mathbf{p}_0$ anti-node at both ends of the cylinder. Given that the non-propagating modes are excited at the reference plane, it follows that the ratio $\mathbf{p}_0^{(2)} / \mathbf{p}_i^{(2)}$ is small at anti-resonance frequencies compared to the same ratio at resonance frequencies, while the opposite is true for the volume velocity, i.e. $\mathbf{U}_0^{(2)} / \mathbf{U}_i^{(2)}$ is large at an anti-resonance and small at a resonance. Hence at anti-resonance, the plane-wave component $\mathbf{Z}_{00}^{(2)}$ of the impedance is relatively small in relation to the other elements $\mathbf{Z}_{ij}$ of the impedance matrix. Since $\mathbf{Z}^{(1)}$ is related to $\mathbf{Z}^{(2)}$ by [3]:

$$\mathbf{Z}^{(1)} = \mathbf{F}\, \mathbf{Z}^{(2)}\, \mathbf{F}^t, \tag{18}$$

where $\mathbf{F}$ is a non-diagonal matrix, it follows that the discrepancy between $\mathbf{Z}_{00}^{(2)}$ and $\mathbf{Z}_{00}^{(1)}$ is larger at anti-resonances than at resonances.

4 CONCLUSIONS AND FUTURE RESEARCH

Accurate measurement of input impedance of an acoustic bore is in principle possible with the TMTC method. We have seen that numerical problems arise precisely in the frequency areas that are predicted by theory; it is known from previous research that such problems can easily be avoided by using different microphone distances and calibration object dimensions. In the case where the calibration objects have the same diameter as the measurement cylinder, the impedance Z measured is that at the reference plane, as seen from the side of the measurement cylinder. If the entry diameter of the acoustic bore under study is also equal to that of the measurement cylinder, than Z is equal to the "plane wave impedance" of the object. In the case where the diameters are not equal, non-propagating modes are excited at the reference plane, and Z does not represent the plane wave impedance of the object. One possible way to solve this problem is to employ calibration objects of the same diameter as the acoustic bore under study; this way the calibration procedure takes into account the effect of the diameter discontinuity. Unfortunately, this approach is not convenient in practice, since different calibration objects would be required for the measurement of objects of different entry diameters. We envisage that a more practicable solution is to predict the effect of the step from equation (18), and take this into account in the derivation of the impedance from the measurements.

REFERENCES

[1] D. B. Sharp, *Acoustic pulse reflectometry for the measurement of musical wind instruments*, Ph.D. thesis, Department of Physics and Astronomy, University of Edinburgh, 1996.

[2] W. Kausel, "Bore reconstruction from measured acoustical input impedance; equipment, signal processing, algorithms and prerequisites," in *Proceedings of the 2001 International Symposium on Musical Acoustics*, Perugia, Italy, 2001, pp. 373-378, The Musical and Architectural Acoustics Laboratory FSSG-CNR, Venezia, Italia.

[3] V. Pagneux, N. Amir, and J. Kergomard, "A study of wave propagation in varying cross-section waveguides by modal decomposition. Part I: Theory and validation," *Journal of the Acoustical Society of America*, vol. 100, no. 4, pp. 2034-2048, 1996.

[4] N. Gibiat and F. Laloë, "Acoustical impedance measurements by the two-microphone-three-calibration (tmtc) method," *Journal of the Acoustical Society of America*, vol. 6, pp. 2533-2544, 1990.

[5] N. H. Fletcher and T. D Rossing, *The Physics of Musical Instruments*, Springer-Verlag, New York, 1991, Second Edition: 1998.

[6] D. H. Keefe, "Woodwind air column models," *Journal of the Acoustical Society of America*, vol. 88, no. 1, pp. 35-51, 1990.

FIGURES

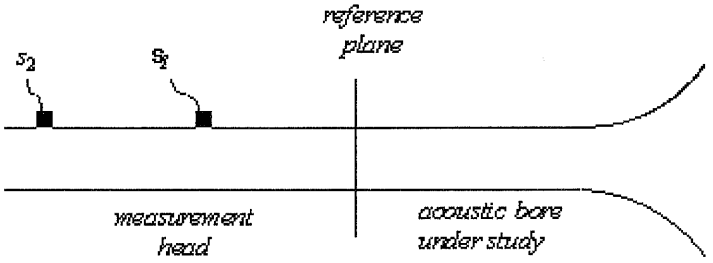

Figure 1: Schematic view of the experimental setup of the TMTC method (after Gibiat and Laloë [4].

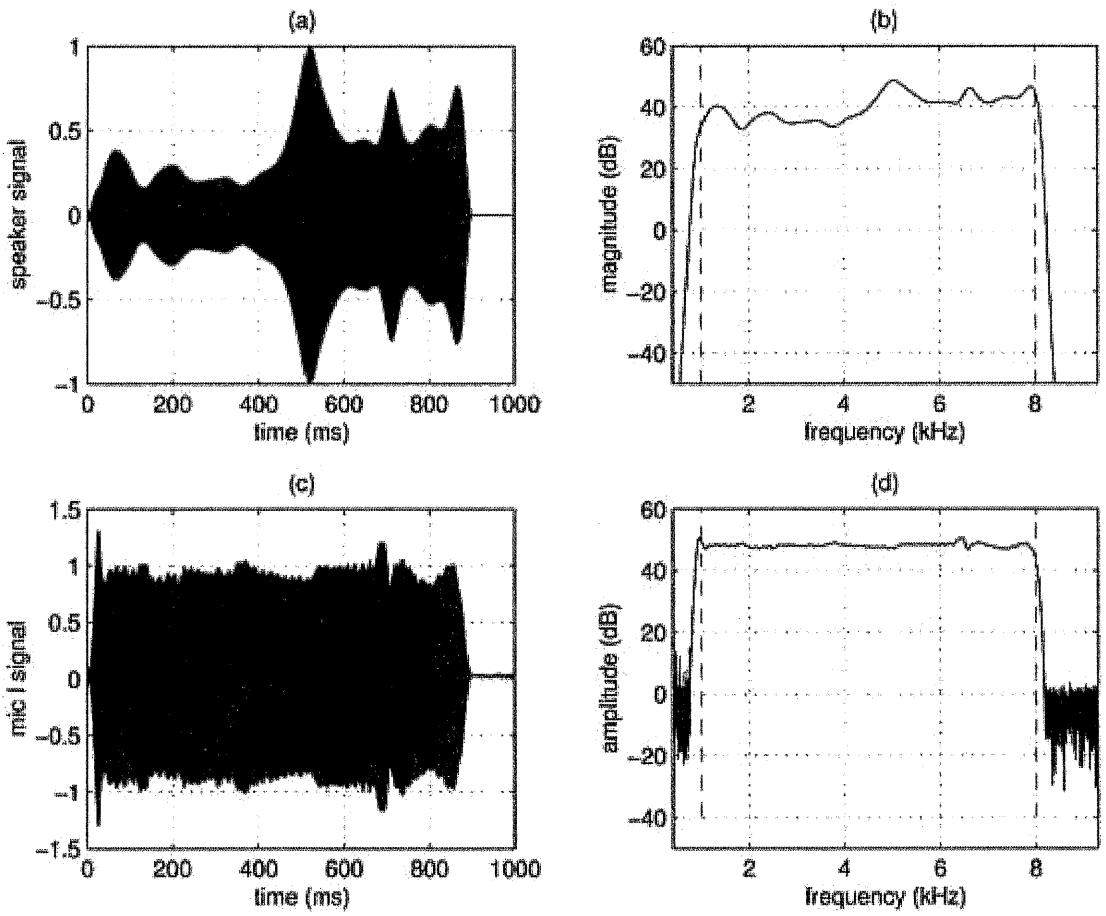

Figure 2: (a): The calibrated chirp signal $h(t)$ that is sent to the speaker. (b): The magnitude of the Fourier transform of $h(t)$. (c): The signal $s_1(t)$ recorded by the microphone. (d): The magnitude of the Fourier transform of $s_1(t)$.

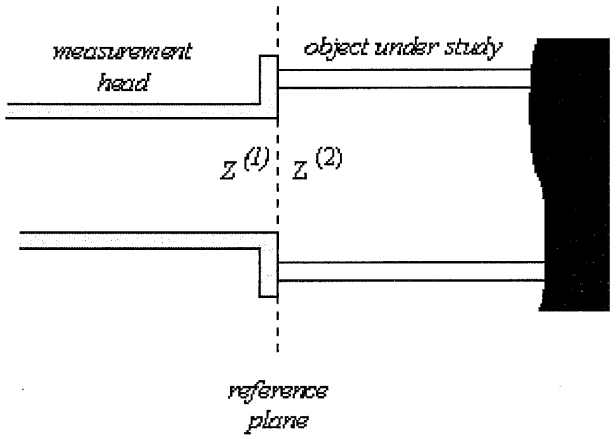

Figure 3: Schematic view of the discontinuity at the reference plane when measuring an object of a larger diameter than the measurement head.

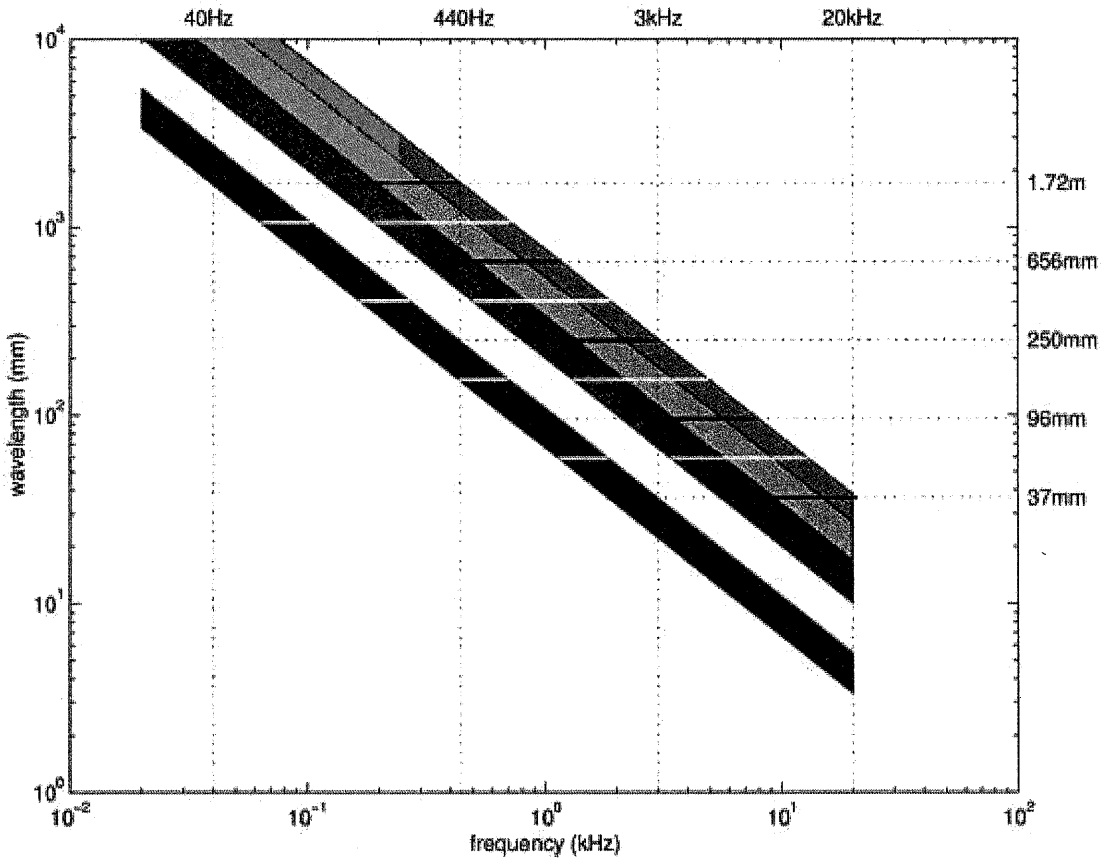

Figure 4: Wavelength versus frequency in the perspective of microphone arrangement. The horizontal solid black line indicate the microphone distance from the first microphone. The horizontal solid yellow lines indicate the "additional" microphone distances. The blue "band" indicates the region between 0.20λ and 0.32λ, and the red, the light-blue, and the green band indicate similar "optimum" regions close to suitable multiples of 0.25λ.

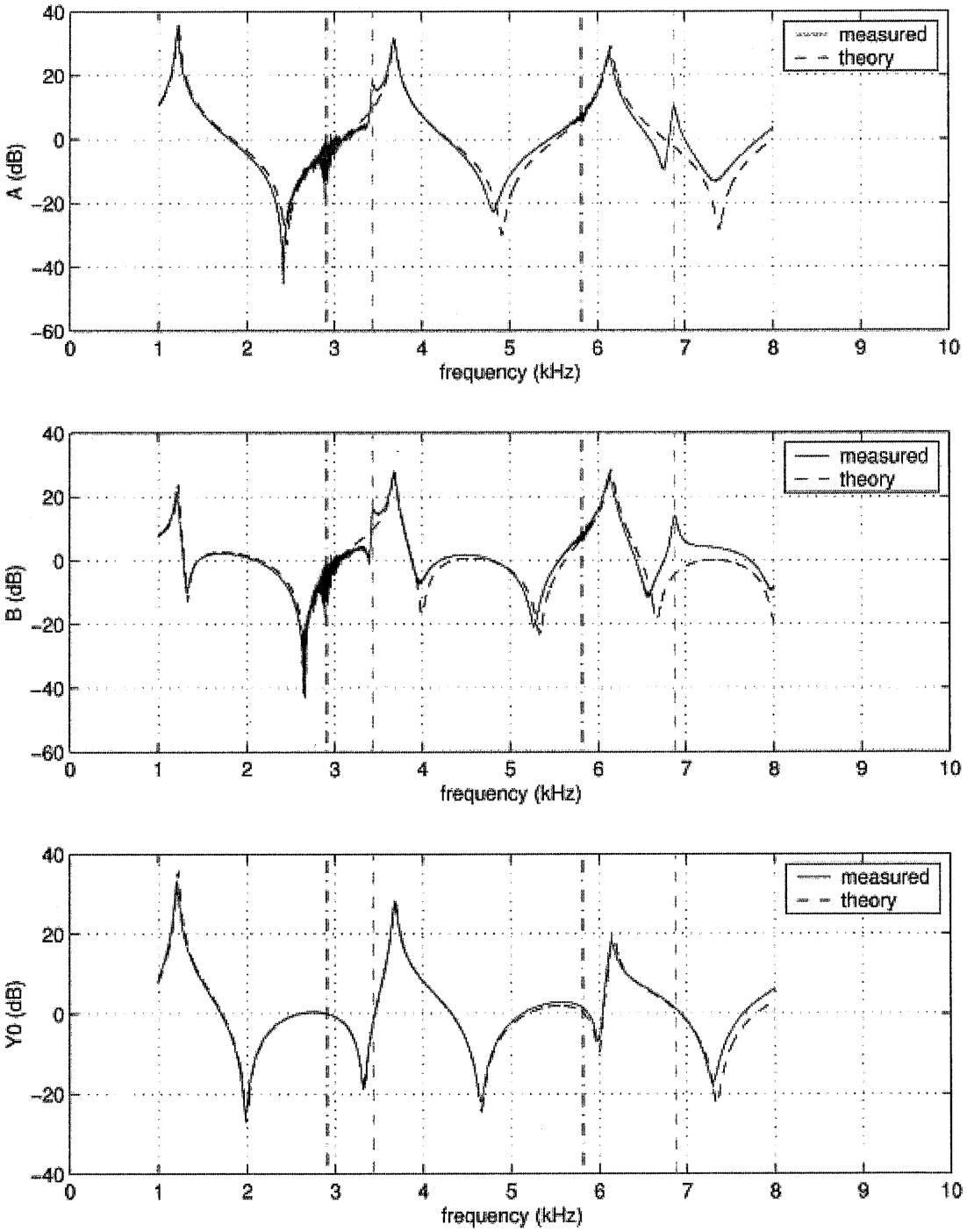

Figure 5: Magnitude of the dimensionless calibration parameters A ,B, and y_0, as derived from measurements using a microphone distance d = 59 mm. The green dashed lines and the black dot-dash lines respectively indicate the frequencies at which L' and d equal half the wavelength.

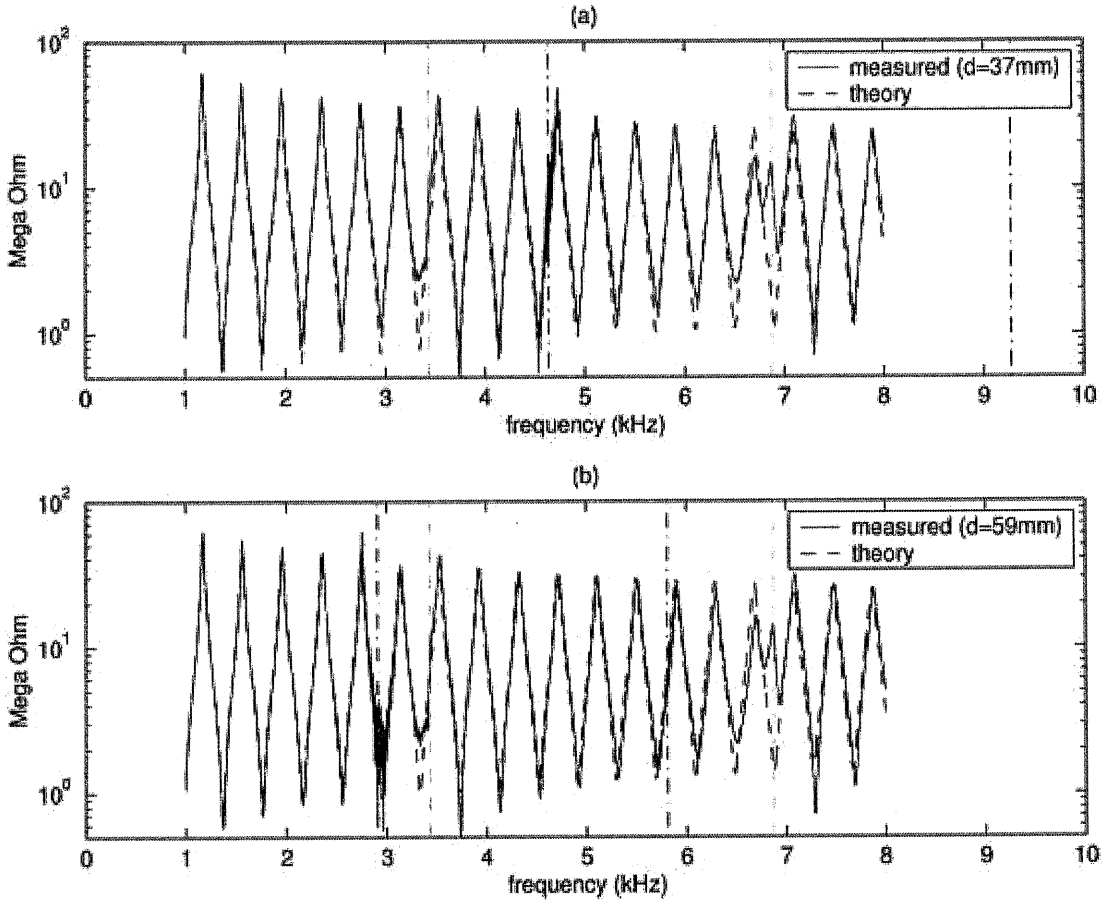

Figure 6: (a): Input impedance of pipe #1, using d = 37 mm. (d): Input impedance of the same pipe, using d = 59 mm. The green dashed lines and the black dot-dash lines respectively indicate the frequencies at which L' and d equal half the wavelength.

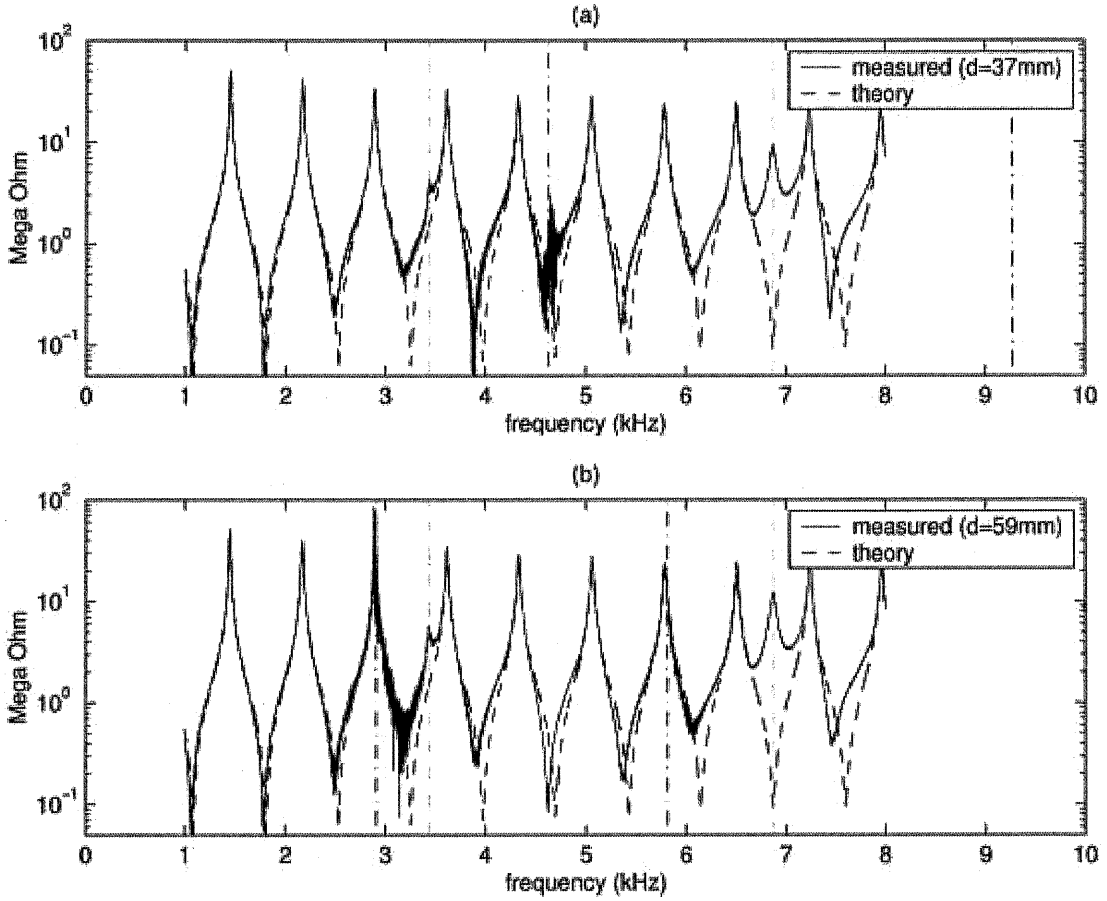

Figure 7: (a): Input impedance of pipe #2, using d = 37 mm. (d): Input impedance of the same pipe, using d = 59 mm. The green dashed lines and the black dot-dash lines respectively indicate the frequencies at which L' and d equal half the wavelength.